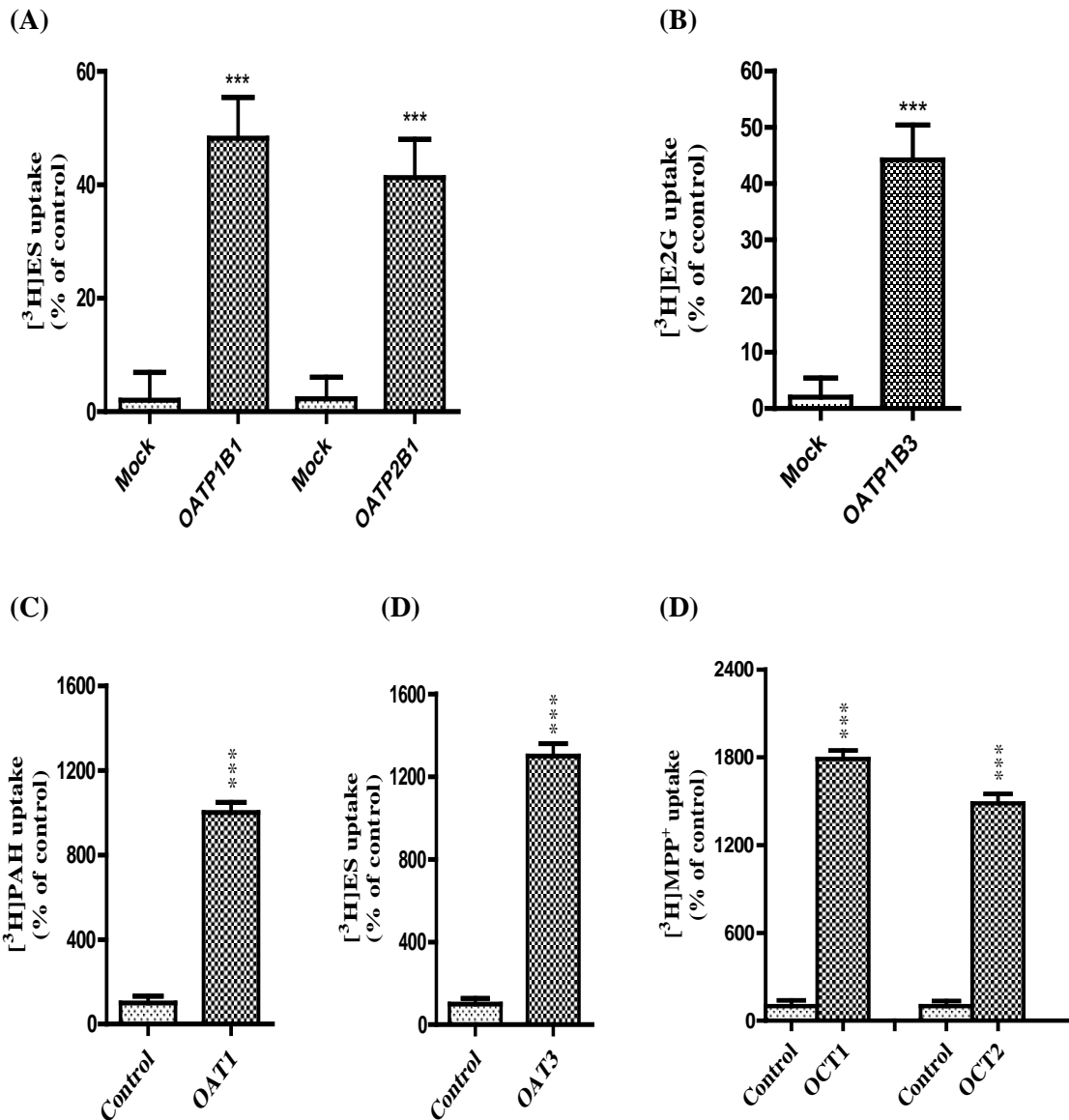
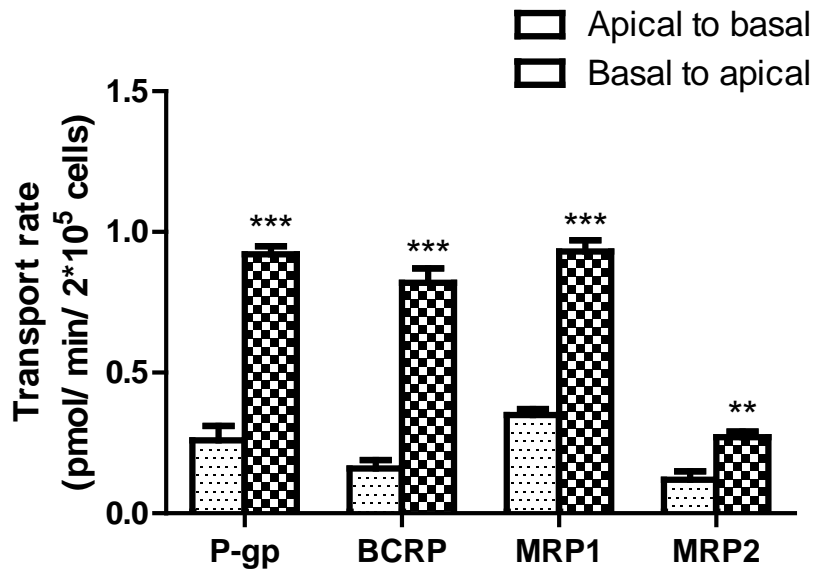


## Supplementary figure 1



**Figure S1.** Characterization of HEK cell stably transfected with human transporters. (A) Intracellular uptake of 45nM  $[^3\text{H}]\text{ES}$  in HEK-OATP1B1 (A), 45nM  $[^3\text{H}]\text{ES}$  in HEK-OATP2B1 (B),  $[^3\text{H}]\text{E2G}$  in HEK-OATP1B3 (C), 89nM  $[^3\text{H}]\text{PAH}$  in HEK-OAT1 (D), 45nM  $[^3\text{H}]\text{ES}$  in HEK-OAT3 (E) and 25nM  $[^3\text{H}]\text{MPP}^+$  in HEK-OCT1 and HEK-OCT2 cells. The uptake amount was determined by subtracting the total amount of uptake in control cells from the uptake in OAT and OCT transporter-expressing cells which was expressed as % of control. Data are presented as the means  $\pm$ SDs from three or more independent experiments. Significant differences compared with the percent uptake for the control (no inhibitor) are indicated (\*\*\*,  $P > 0.001$ ).

## Supplementary figure 2



**Figure S2.** Transepithelial transport of probe substrate for P-gp, BCRP, MRP1 and MRP2-cells. The apical to basal and basal to apical transport of 50nM digoxin (P-gp), 24nM prazosin (BCRP), 45nM estrone sulphate (MRP1), and 24 nM vinblastin (MRP2) across LLCPK-MDR1, LLCPK-BCRP and MDCKII-MRP1, MDCKII-MRP2 cell monolayers. Each data point presents the means  $\pm$ SDs of three or more independent experiments. Significant differences compared with the percent uptake for the control (no inhibitor) are indicated (\*\*,  $P > 0.01$ ; \*\*\*,  $P > 0.001$ ).

### Supplementary figure 3

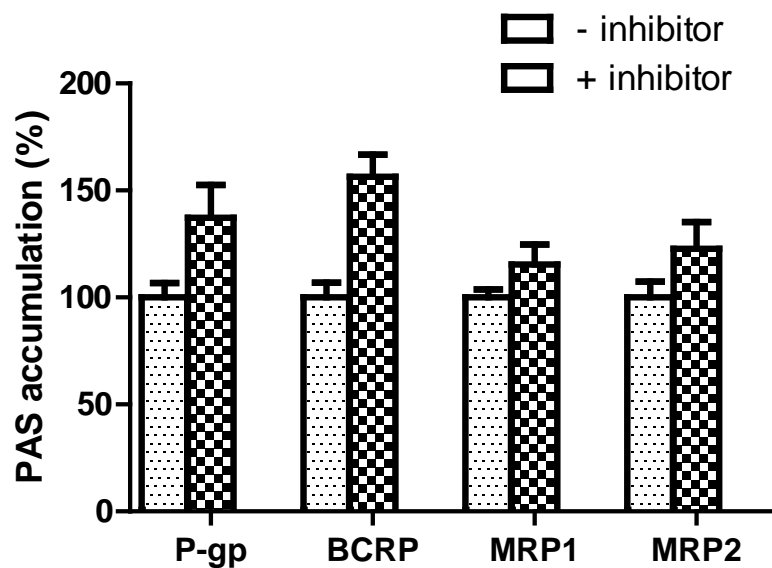


**Figure S3.** Cellular accumulation of PAS in ABC efflux transporters. The accumulation of 10  $\mu$ M PAS was measured in presence or absence of 20  $\mu$ M verapamil for P-gp, 20  $\mu$ M rosuvastatin for BCRP, 20  $\mu$ M MK571 for MRP1 and MRP2 across LLCPK-MDR1, LLCPK-BCRP and MDCKII-MRP1, MDCKII-MRP2 cells. Each data point presents the means  $\pm$ SDs of three or more independent experiments.

**Supplementary table 1.** Cellular uptake of *in vitro* radiolabeled prototype substrates into stably transfected HEK-OATP1B1, HEK-OATP2B1, HEK-1B3, HEK-OAT1, HEK-OAT3, HEK-OCT1 and HEK-OCT2 cells <sup>a</sup>.

Substrate <sup>b</sup>	Transporter	$K_m$ ( $\mu\text{M}$ )	$V_{max}$ (pmol/min/ mg protein)	$Cl_{int}$ ( $\mu\text{l}/\text{min}/\text{mg}$ protein)	Reported $K_m$ ( $\mu\text{M}$ ) <sup>c</sup>
[ <sup>3</sup> H]ES	OATP1B1	2.3	28.0	12.17	2.4(1), 12.5(2)
[ <sup>3</sup> H]ES	OATP2B1	5.8	32.0	6.4	7.1(3), 8.09(4),10.2(5)
[ <sup>3</sup> H]E2G	OATP1B3	8.4	12.0	1.52	15.8(1), 24.6(6)
[ <sup>3</sup> H]PAH	OAT1	23.9	517.8	21.7	28(7), 15.4(8)
[ <sup>3</sup> H]ES	OAT3	7.6	130.6	17.2	6.3(7)
[ <sup>3</sup> H]MPP <sup>+</sup>	OCT1	17.0	132.6	7.80	14.6(9), 21(10)
[ <sup>3</sup> H]MPP <sup>+</sup>	OCT2	21.0	515.5	24.5	16 (11), 19.5 (12)

<sup>A</sup> Shown are the intracellular uptake kinetics of the cells derived from *in vitro* experiments:  $K_m$ , Michelis-Menten constant;  $V_{max}$ , maximum rate of uptake;  $CL_{int}$ , intrinsic clearance per unit of time. Data represent the mean values from triplicate experiments.

<sup>b</sup> [<sup>3</sup>H]-estrone sulphate for OATP1B1 and OATP2B1, [<sup>3</sup>H]-estradiol 17 $\beta$ -D-glucuronide, [<sup>3</sup>H]-para-aminohippurate ([<sup>3</sup>H]-PAH) for OAT1, [<sup>3</sup>H]-estrone-3-sulfate ([<sup>3</sup>H]-ES ) for OAT3 and [<sup>3</sup>H] N-methyl-4-phenylpyridinium ([<sup>3</sup>H]-MPP<sup>+</sup>) for OCT1 and OCT2 with the substrate in a concentration range of 0.1-100  $\mu\text{M}$  were normalized to the control and used to determine cell function.

<sup>c</sup> Reported  $K_m$  values represent previously published reference data from the references cited in parentheses

## Supplementary figure 4

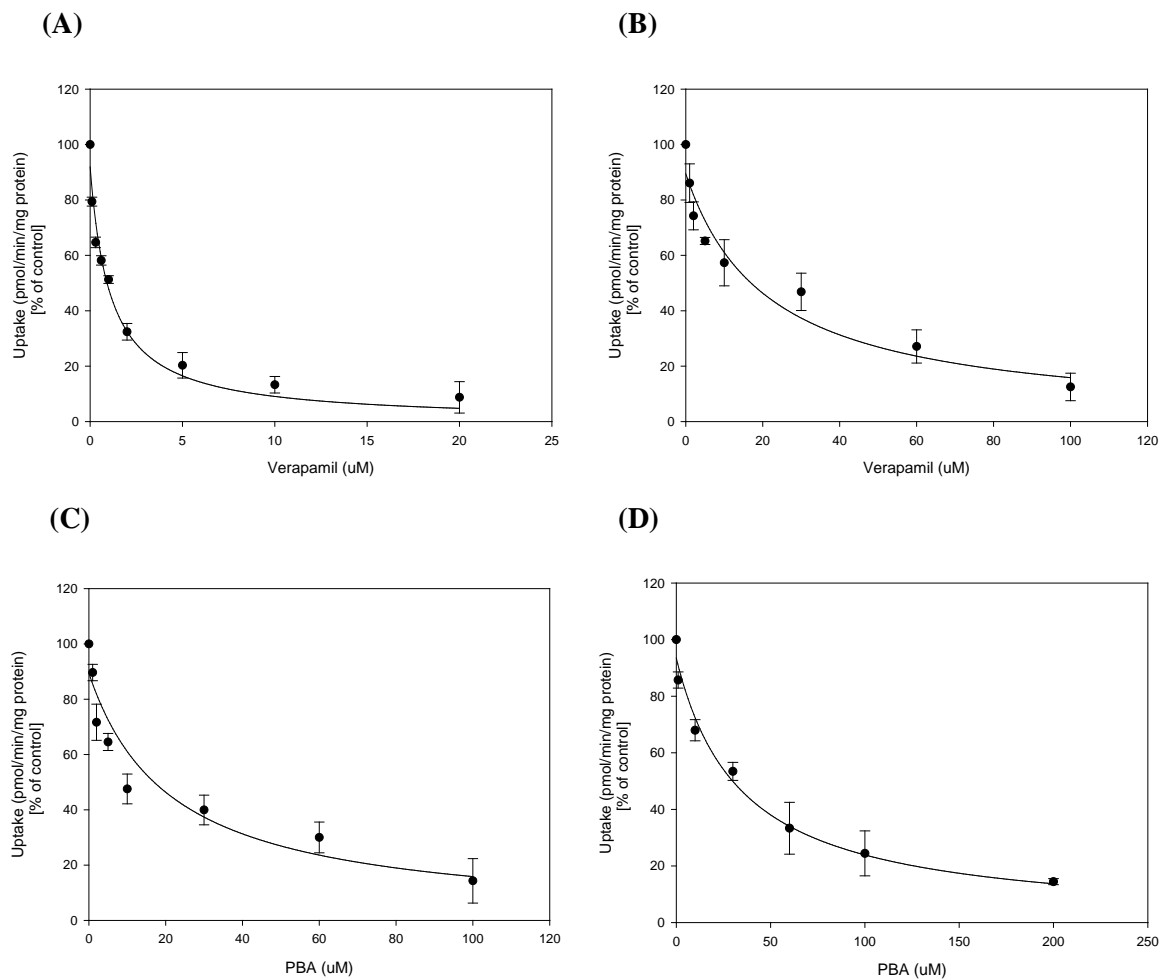


Figure S4. Concentration dependent inhibition of PAS Uptake in (A) hOCT1 overexpressed HEK293 cells by Verapamil (B) hOCT2 by Verapamil, (C) hOAT1 by Probenecid, (D) hOAT3 by Probenecid. All the data showed relative to control (no inhibitor) and mean  $\pm$ SDs of triplicate of experiment.

**Supplementary table 2.** Kinetic parameters of inhibitors used for the calculation of R-values

$[I]_{u,inlet,max}$  (estimated maximum unbound inhibitor concentrations at the inlet to the liver) of anti-TB drugs, were calculated by the equation, as described under *Materials and Methods*, in which  $k_a$  of 0.1 min<sup>-1</sup>,  $F_a \times F_g$  of 1, and  $Q_h$  of 1500mL/min were used. The blood to plasma concentration ratios of the inhibitors were assumed to be unity in the  $[I]_{u,inlet,max}$  calculations.

Drugs	Dose	Fu	C <sub>max</sub>	C <sub>max,u</sub>
	mg		μM	μM
Probenecid	1000	0.15(13)	243.9(13)	36.6
Verapamil	180	0.1(14)	0.55(14)	0.055
Ibuprofen	800	0.01(15)*	266.1(15)	2.66
Indomethacin	75	0.01(16)*	4.05(16)	0.040
Diclofenac	50	0.004(17)	9.42(17)	0.045
Naproxen	250	0.01(18)*	270.1(18)	2.70
Omeprazole	20	0.03(19)	3.12(20)	0.10
Lansoprazole	30	0.03(21)	4.87(22)	0.150
Cimetidine	400	0.8(23)	9352(24)	7481
Metformin	500	1(25)	10.99(26)	10.99
Quinidine	325	0.5(27)	13.56(28)	6.78
Rifampin	600	0.15(29)	23.0(30)	3.45

\*Asterisk indicates an arbitrary 1% free fraction was used according to the FDA draft guidance for drug interaction prediction to avoid false prediction.

## References

1. **Gui C, Miao Y, Thompson L, Wahlgren B, Mock M, Stieger B, Hagenbuch B.** 2008. Effect of pregnane X receptor ligands on transport mediated by human OATP1B1 and OATP1B3. *Eur J Pharmacol* **584**:57-65.
2. **Cui Y, Konig J, Leier I, Buchholz U, Keppler D.** 2001. Hepatic uptake of bilirubin and its conjugates by the human organic anion transporter SLC21A6. *J Biol Chem* **276**:9626-9630.
3. **Satoh H, Yamashita F, Tsujimoto M, Murakami H, Koyabu N, Ohtani H, Sawada Y.** 2005. Citrus juices inhibit the function of human organic anion-transporting polypeptide OATP-B. *Drug Metab Dispos* **33**:518-523.
4. **Nozawa T, Imai K, Nezu J, Tsuji A, Tamai I.** 2004. Functional characterization of pH-sensitive organic anion transporting polypeptide OATP-B in human. *J Pharmacol Exp Ther* **308**:438-445.
5. **Noe J, Portmann R, Brun ME, Funk C.** 2007. Substrate-dependent drug-drug interactions between gemfibrozil, fluvastatin and other organic anion-transporting peptide (OATP) substrates on OATP1B1, OATP2B1, and OATP1B3. *Drug Metab Dispos* **35**:1308-1314.
6. **Hirano M, Maeda K, Shitara Y, Sugiyama Y.** 2004. Contribution of OATP2 (OATP1B1) and OATP8 (OATP1B3) to the hepatic uptake of pitavastatin in humans. *J Pharmacol Exp Ther* **311**:139-146.
7. **Ueo H, Motohashi H, Katsura T, Inui K.** 2005. Human organic anion transporter hOAT3 is a potent transporter of cephalosporin antibiotics, in comparison with hOAT1. *Biochem Pharmacol* **70**:1104-1113.
8. **Cihlar T, Ho ES.** 2000. Fluorescence-based assay for the interaction of small molecules with the human renal organic anion transporter 1. *Anal Biochem* **283**:49-55.
9. **Zhang L, Dresser MJ, Gray AT, Yost SC, Terashita S, Giacomini KM.** 1997. Cloning and functional expression of a human liver organic cation transporter. *Mol Pharmacol* **51**:913-921.
10. **Bachmakov I, Glaeser H, Fromm MF, Konig J.** 2008. Interaction of oral antidiabetic drugs with hepatic uptake transporters: focus on organic anion transporting polypeptides and organic cation transporter 1. *Diabetes* **57**:1463-1469.
11. **Busch AE, Karbach U, Miska D, Gorboulev V, Akhoundova A, Volk C, Arndt P, Ulzheimer JC, Sonders MS, Baumann C, Waldegger S, Lang F, Koepsell H.** 1998. Human neurons express the polyspecific cation transporter hOCT2, which translocates monoamine neurotransmitters, amantadine, and memantine. *Mol Pharmacol* **54**:342-352.
12. **Zolk O, Solbach TF, Konig J, Fromm MF.** 2009. Structural determinants of inhibitor interaction with the human organic cation transporter OCT2 (SLC22A2). *Naunyn Schmiedebergs Arch Pharmacol* **379**:337-348.
13. **Selen A, Amidon GL, Welling PG.** 1982. Pharmacokinetics of probenecid following oral doses to human volunteers. *J Pharm Sci* **71**:1238-1242.
14. **van Haarst AD, Dijkmans AC, Weimann HJ, Kemme MJ, Bosch JJ, Schoemaker RC, Cohen AF, Burggraaf J.** 2009. Clinically important interaction between tedisamil and verapamil. *J Clin Pharmacol* **49**:560-567.
15. **el-Sayed YM, Gouda MW, al-Khamis KI, al-Meshal MA, al-Dhawali AA, al-Rayes S, Bin-Salih SA, al-Rashood KA.** 1995. Comparative bioavailability of two tablet formulations of ibuprofen. *Int J Clin Pharmacol Ther* **33**:294-298.
16. **Alqahtani S, Kaddoumi A.** 2015. Development of Physiologically Based Pharmacokinetic/Pharmacodynamic Model for Indomethacin Disposition in Pregnancy. *PLoS One* **10**:e0139762.

17. **Mustofa M, Suryawati S, Dwiprahasto I, Santoso B.** 1991. The relative bioavailability of diclofenac with respect to time of administration. *Br J Clin Pharmacol* **32**:246-247.
18. **Vree TB, Van Den Biggelaar-Martea M, Verwey-Van Wissen CP, Vree ML, Guelen PJ.** 1993. The pharmacokinetics of naproxen, its metabolite O-desmethylnaproxen, and their acyl glucuronides in humans. Effect of cimetidine. *British Journal of Clinical Pharmacology* **35**:467-472.
19. **Cederberg C, Andersson T, Skanberg I.** 1989. Omeprazole: pharmacokinetics and metabolism in man. *Scand J Gastroenterol Suppl* **166**:33-40; discussion 41-32.
20. **Regårdh CG, Andersson T, Lagerström PO, Lundborg P, Skånberg I.** 1990. The Pharmacokinetics of Omeprazole in Humans-A Study of Single Intravenous and Oral Doses. *Therapeutic Drug Monitoring* **12**:163-172.
21. **Masa K, Hamada A, Arimori K, Fujii J, Nakano M.** 2001. Pharmacokinetic differences between lansoprazole enantiomers and contribution of cytochrome P450 isoforms to enantioselective metabolism of lansoprazole in dogs. *Biol Pharm Bull* **24**:274-277.
22. **Ieiri I, Kishimoto Y, Okochi H, Momiyama K, Morita T, Kitano M, Morisawa T, Fukushima Y, Nakagawa K, Hasegawa J, Otsubo K, Ishizaki T.** 2001. Comparison of the kinetic disposition of and serum gastrin change by lansoprazole versus rabeprazole during an 8-day dosing scheme in relation to CYP2C19 polymorphism. *Eur J Clin Pharmacol* **57**:485-492.
23. **Kalvass JC, Maurer TS, Pollack GM.** 2007. Use of Plasma and Brain Unbound Fractions to Assess the Extent of Brain Distribution of 34 Drugs: Comparison of Unbound Concentration Ratios to in Vivo P-Glycoprotein Efflux Ratios. *Drug Metabolism and Disposition* **35**:660-666.
24. **Somogyi A, Stockley C, Keal J, Rolan P, Bochner F.** 1987. Reduction of metformin renal tubular secretion by cimetidine in man. *British Journal of Clinical Pharmacology* **23**:545-551.
25. **Chu X, Korzekwa K, Elsby R, Fenner K, Galetin A, Lai Y, Matsson P, Moss A, Nagar S, Rosania GR, Bai JPF, Polli JW, Sugiyama Y, Brouwer KLR, on behalf of the International Transporter C.** 2013. Intracellular Drug Concentrations and Transporters: Measurement, Modeling, and Implications for the Liver. *Clinical pharmacology and therapeutics* **94**:126-141.
26. **Song IS, Shin HJ, Shim EJ, Jung IS, Kim WY, Shon JH, Shin JG.** 2008. Genetic variants of the organic cation transporter 2 influence the disposition of metformin. *Clin Pharmacol Ther* **84**:559-562.
27. **Ochs HR, Greenblatt DJ, Woo E.** 1980. Clinical Pharmacokinetics of Quinidine. *Clinical Pharmacokinetics* **5**:150-168.
28. **Rakhit A, Holford NH, Guentert TW, Maloney K, Riegelman S.** 1984. Pharmacokinetics of quinidine and three of its metabolites in man. *J Pharmacokinet Biopharm* **12**:1-21.
29. **Burman WJ, Gallicano K, Peloquin C.** 2001. Comparative pharmacokinetics and pharmacodynamics of the rifamycin antibacterials. *Clin Pharmacokinet* **40**:327-341.
30. **Maeda K, Ikeda Y, Fujita T, Yoshida K, Azuma Y, Haruyama Y, Yamane N, Kumagai Y, Sugiyama Y.** 2011. Identification of the rate-determining process in the hepatic clearance of atorvastatin in a clinical cassette microdosing study. *Clin Pharmacol Ther* **90**:575-581.